THE JOURNAL OF BIOLOGICAL CHEMISTRY
Vol. 278, No. 43, Issue of October 24, pp. 42435–42440, 2003
Printed in U.S.A.

Two Aspartic Acid Residues in the PSST-Homologous NUKM Subunit of Complex I from *Yarrowia lipolytica* Are Essential for Catalytic Activity*

Received for publication, June 3, 2003, and in revised form, August 8, 2003
Published, JBC Papers in Press, August 20, 2003, DOI 10.1074/jbc.M305819200

Aurelio Garofano, Klaus Zwicker, Stefan Kerscher, Pamela Okun‡, and Ulrich Brandt§

From the Johann Wolfgang Goethe-Universität Frankfurt am Main, Fachbereich Medizin, Gustav Embden Zentrum der Biologischen Chemie, Institut für Biochemie I, Theodor-Stern-Kai 7, Haus 25B, D-60590 Frankfurt am Main, Germany

Mitochondrial proton-translocating NADH:ubiquinone oxidoreductase (complex I) couples the transfer of two electrons from NADH to ubiquinone to the translocation of four protons across the mitochondrial inner membrane. Subunit PSST is the most likely carrier of iron-sulfur cluster N2, which has been proposed to play a crucial role in ubiquinone reduction and proton pumping. To explore the function of this subunit we have generated site-directed mutants of all eight highly conserved acidic residues in the *Yarrowia lipolytica* homologue, the NUKM protein. Mutants D99N and D115N had only 5 and 8% of the wild type catalytic activity, respectively. In both cases complex I was stably assembled but electron paramagnetic resonance spectra of the purified enzyme showed a reduced N2 signal (about 50%). In terms of complex I catalytic activity, almost identical results were obtained when the aspartates were individually changed to glutamates or to glycines. Mutations of other conserved acidic residues had less dramatic effects on catalytic activity and did not prevent assembly of iron-sulfur cluster N2. This excludes all conserved acidic residues in the PSST subunit as fourth ligands of this redox center. The results are discussed in the light of the structural similarities to the homologous small subunit of water-soluble [NiFe] hydrogenases.

Proton-translocating NADH:ubiquinone oxidoreductase (complex I) is the first of five complexes of oxidative phosphorylation in the mitochondrial inner membrane. In complex I, two electrons are transported from NADH to ubiquinone via FMN and eight iron-sulfur clusters (1). In this process four protons are translocated across the membrane (2). The mechanism of this process and the location and nature of the ubiquinone binding sites are still unclear (3). Evidence obtained with bovine heart submitochondrial particles strongly suggests that iron-sulfur cluster N2 is directly involved in ubiquinone reduction: based on paramagnetic interaction, the distance between an ubisemiquinone radical and cluster N2 was estimated to be 8–11 Å (4). Subunit PSST is the most likely carrier of iron-sulfur cluster N2. Site-directed mutagenesis of the homologue subunits in *Escherichia coli* (5) and *Neurospora crassa* (6) indicated that three cysteines of subunit PSST are ligands for cluster N2. These cysteines correspond to positions 86, 150, and 180 in the PSST homologous NUKM subunit of *Yarrowia lipolytica*. A glutamate residue (Glu-89 in *Y. lipolytica*) had been proposed as the fourth ligand (7), but this could be excluded by site-directed mutagenesis (8). Thus, the fourth ligand of cluster N2 is still not known. Albracht and co-workers (9) have proposed that complex I contains two iron-sulfur clusters N2 that have identical electron paramagnetic resonance (EPR) spectra and are bound by the two ferredoxin-like Fe_4S_4 binding motifs in the TYKY subunit. However, these two clusters in the TYKY subunit have been shown to be EPR-silent and designated N6a and N6b by Friedrich and co-workers (10). Ubiquinone-analogous complex I inhibitors like 2-decyl-4-quinazolinyl amine (DQA),[1] rotenone, and pyridaben are thought to prevent the terminal electron transfer step from cluster N2 to ubiquinone (7). Using a trifluoromethyl derivative of pyridaben for photoaffinity labeling, the PSST subunit was identified as high-affinity target (11), suggesting that this subunit is in close vicinity to the ubiquinone binding site of complex I.

It has been known for a long time that complex I is evolutionary related to [NiFe] hydrogenases (12, 13). The [NiFe] hydrogenase from *Desulfovibrio fructosovorans* is a water soluble enzyme for which the molecular structure has been solved (24, 26). This enzyme consists of a large and a small subunit. The small subunit carries three iron-sulfur clusters, and part of its sequence is homologous to subunit PSST. The large subunit contains the [NiFe] cluster, and its sequence is homologous to the 49-kDa subunit of complex I. Based on a site-directed mutagenesis study in *Y. lipolytica*, it has been proposed that the ubiquinone-reactive catalytic core of complex I has directly evolved from the catalytic center of [NiFe] hydrogenases and that critical parts of the structural fold have been retained during evolution (14). According to this model a significant part of the ubiquinone binding site and iron-sulfur cluster N2 are predicted to reside at the interface between the 49-kDa and PSST subunits of complex I (15). To search for the fourth ligand of iron-sulfur cluster N2 and to identify functionally important amino acids in subunit PSST, we have constructed and characterized mutants for all highly conserved acidic residues in the homologous subunit of *Y. lipolytica*, the NUKM protein.

MATERIALS AND METHODS

Substrates and Inhibitors—n-decylubiquinone (DBQ), deamino-NADH (dNADH), hexa-ammine-ruthenium(III)-chloride (HAR), and rotenone were purchased from Sigma, hygromycin B from Invitrogen, and

* This work was supported by the Deutsche Forschungsgemeinschaft, Sonderforschungsbereich 472, P2 and the Fonds der Chemischen Industrie. The costs of publication of this article were defrayed in part by the payment of page charges. This article must therefore be hereby marked "*advertisement*" in accordance with 18 U.S.C. Section 1734 solely to indicate this fact.

‡ Present address: Universität Heidelberg, Molekulare Evolution und Genomik, Im Neuenheimer Feld 230, D-69120 Heidelberg, Germany.

§ To whom correspondence should be addressed: Universität Frankfurt, Fachbereich Medizin, Institut für Biochemie I, Theodor-Stern-Kai 7, Haus 25B, D-60590 Frankfurt am Main, Germany. Tel.: 49-69-6301-6926; Fax: 49-69-6301-6970; E-mail: brandt@zbc.kgu.de.

[1] The abbreviations used are: DQA, 2-decyl-4-quinazolinyl amine; DBQ, n-decylubiquinone; dNADH, deamino-nicotinamide-adenine-dinucleotide; EPR, electron paramagnetic resonance; HAR, hexa-ammine-ruthenium(III)-chloride; Mes, 4-morpholineethanesulfonic acid; Mops, 4-morpholinepropanesulfonic acid.

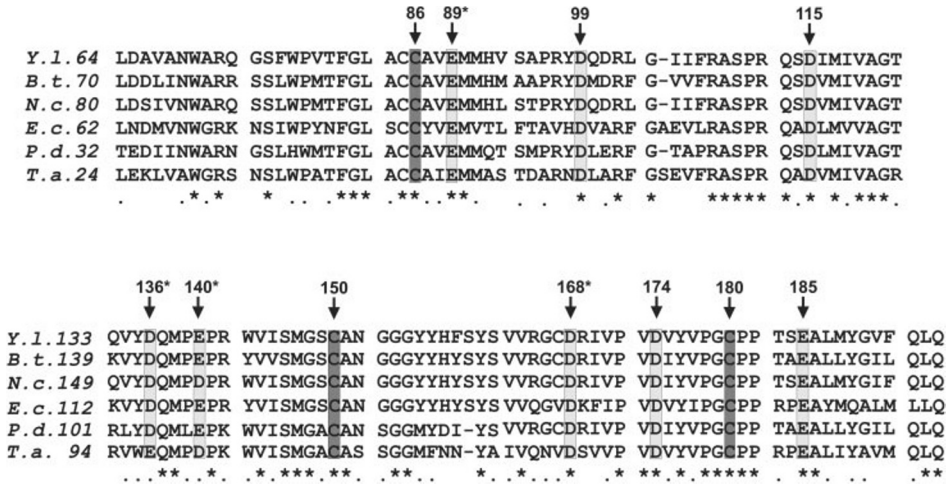

FIG. 1. **Alignment of PSST-homologous subunits of complex I.** Identical amino acids are marked by *asterisks*, similar residues by *dots*. Proposed ligands for Fe_4S_4 cluster N2 are shaded in *dark gray*, conserved acidic amino acids are shaded in *light gray* and *labeled* with their number in the sequence of the *Y. lipolytica* protein. *Y.l., Yarrowia lipolytica; B.t., Bos taurus; N.c., Neurospora crassa; E.c., Escherichia coli; P.d., Paracoccus denitrificans; T.a., Thermus aquaticus*. Mutants in positions Glu-89, Asp-136, Glu-140, and Asp-168 were described in Ref. 8.

DQA was a generous gift from Aventis CropScience, Frankfurt am Main (Germany).

Strains—*Y. lipolytica* strains E129 (*MatB*, *lys 11*-23, *ura3*-302, *leu2*-270, *xpr2*-322) and E150 (*Mat*A, *his*-1, *ura3*-302, *leu2*-270, *xpr2*-322) were a kind gift from Prof. C. Gaillardin (Institute National de la Recherche Agronomique, Paris, France). Complex I deletion strains could be generated after redirecting the alternative NADH dehydrogenase (NDH2) to the matrix site (16). The internal version of NDH2 (NDH2i) rescues complex I deficiency, allowing the survival of mutants lacking complex I function. The *NUKM* gene was deleted by homologous recombination with a *LEU2*-marked deletion allele (8). To purify complex I by Ni^{2+} affinity chromatography, a six alanine spacer plus a His_6 tag was attached to the C terminus of the NUGM (30 kDa) subunit (17) and integrated at the *NUGM* locus by pop-in-pop-out recombination (18). The two strains were conjugated, and the resulting diploid strain was sporulated to obtain a strain with both the *NUGM*-tag and the *nukm*::*LEU2* alleles. *LEU*2^+ spores were tested for the absence of the genomic copy of *NUKM* using the polymerase chain reaction PCR and Southern blotting.

Site-directed Mutagenesis of NUKM—Point mutations were created using the QuikChange site-directed mutagenesis method from Stratagene, using as template a 2.3-kb *Eco*RI genomic fragment from the *NUKM* locus, subcloned into the replicative vector pUB4 carrying the *HygB*^{R} resistance gene. Mutated plasmids were confirmed by DNA sequencing and used for transformation of the deletion strain *nukm*::*LEU2-NUGM*-tag. Transformants were selected by hygromycin B resistance, and the mutation was reconfirmed by sequencing of the entire open reading frame on the plasmid. The mutations were analyzed in comparison to the pUB4 complemented deletion strain *nukm*::*LEU2-NUGM*-tag as parental strain.

Purification of Complex I—Unsealed mitochondrial membranes were prepared from parental and mutant haploid strains (*nukm*::*LEU2*, *ura3, leu2, lys11*, pUB4-$nukm_{mut}$/*Hyg*) as described previously (17, 19). Complex I was purified by extraction of mitochondrial membranes with dodecyl maltoside followed by Ni^{2+}-agarose and size exclusion chromatography (17). Affinity purification of His-tagged complex I, followed by gel filtration, gave pure enzyme (~95%) with a total yield of 38% for the parental strain. Blue native polyacrylamide gel electrophoresis was performed as described in Ref. 20.

EPR Spectroscopy—Low temperature EPR spectra were obtained on a Bruker ESP 300E spectrometer equipped with a liquid helium continuous flow cryostat, ESR 900 from Oxford Instruments. Samples of purified complex I were mixed with NADH in the EPR tube and frozen in liquid nitrogen after 30 s reaction time. Spectra were recorded at 12 K or at 40 K with the following instrument settings: microwave frequency 9.475 GHz, microwave power 1 mW, modulation amplitude 0.64 mT. Under these conditions spectra show contributions from clusters N1, N2, N3, and N4 (21).

Redox Titrations—For redox titrations mitochondrial membranes (~200 mg protein) were sedimented by centrifugation for 1 h at 48,000 × *g*. The pellet was suspended in 30 ml of buffer containing 30 mM each of sodium-acetate, Mes, Mops, Tris, glycine, pH 7.0, 100 mM NaCl, and 1 mM EDTA and centrifuged as before. After one additional washing step the resulting pellet was suspended in 4–5 ml of the above buffer yielding a final protein concentration of 25–30 mg/ml. The following redox mediators were added to a final concentration of 30 μM each: tetramethyl-phenylenediamine, phenazine-methosulfate, methylene blue, menadione, resorufin, indigotrisulfonate, 1,2-naphthoquinone, 2-hydroxy-1,4-naphthoquinone, phenosafranine, benzyl viologen, and methyl viologen. Redox titrations were performed anaerobically as described in Ref. 22. The membrane suspension was poised at appropriate potential values by small additions of freshly prepared 50 mM dithionite. Aliquots were anaerobically transferred into an EPR tube, frozen rapidly in cold isopentane/methylcyclohexane (5:1), and stored in liquid nitrogen.

Cluster N2 reduction rate in the frozen samples was then determined by recording EPR spectra at 12 K from samples poised at redox potentials between +100 and −500 mV. After subtraction of the oxidized spectrum recorded at a redox poise between +30 and −30 mV, to eliminate signal contributions from components with higher redox potential, the intensity of the N2 EPR signal was calculated by scaling it to a simulated N2 spectrum. The resulting N2 reduction rates were fitted to the Nernst equation using PSI Plot (Poly Software International, Salt Lake City, UT).

Activity Measurements—dNADH:DBQ oxidoreductase activity was assayed at 30 °C in a Shimadzu UV-300 spectrophotometer as dNADH oxidation rate ($\epsilon_{340-400\ nm}$ = 6.22 $mM^{-1}\ cm^{-1}$) in the presence of 100 μM dNADH and 50 mM Tris/HCl, pH 7.4, and 2 mM KCN. The reaction was started by the addition of 60 μM DBQ. Inhibitors were added from stock solutions (10 mM in ethanol) prior to DBQ. Michaelis-Menten parameters were determined by varying the concentration of DBQ (2–100 μM), and data were analyzed with the Enzfitter Software-Package (Version 2.0.16.0, Biosoft, Cambridge, UK). Detergent- and inhibitor-insensitive NADH:HAR activity was measured using 200 μM NADH and 2 mM HAR, 2 mM NaN_3 in 20 mM Na^+/Hepes, pH 8.0, at 30 °C (23), and used to quantify the complex I content in the membranes. The reaction was started by the addition of 50 μg (total protein) of unsealed mitochondrial membranes. To test for temperature stability mitochondrial membranes were incubated for 5 mins at increasing temperatures (30–60 °C) before NADH:HAR activity was tested as described at 30 °C.

RESULTS

By alignment of protein sequences of PSST homologous subunits of complex I from different species, eight highly conserved acidic amino acids could be identified (Fig. 1). We have explored their possible role in the catalytic mechanism of complex I by site-directed mutagenesis of the *NUKM* gene in *Y. lipolytica* (*Y. lipolytica* numbering is used throughout, but the bovine name PSST is used in most cases). The resulting mutants were characterized in terms of complex I assembly and function. Data from an earlier study in which we had reported the results from mutagenesis of four of the eight positions (8) are

TABLE I
Characterization of mutants in the PSST homologous NUKM subunit

Strain	Complex I content[a]	V_{max}[b]	K_m	I_{50} rotenone	I_{50} DQA
		$\mu mol\ min^{-1}\ mg^{-1}$	μm	*nm*	*nm*
Parental	1.00	0.40 ± 0.02	22 ± 2	500	20
E89A[c]	1.60	0.43 ± 0.02	19 ± 1	590	13
E89C[c]	1.60	0.39 ± 0.02	18 ± 1	630	14
E89Q[c]	1.10	0.51 ± 0.02	9 ± 1	620	11
D99N	0.90	0.015			
D99E	0.95	0.016			
D99G	0.93	0.015			
D115N	1.05	0.024			
D115E	1.01	0.021			
D115G	1.04	0.023			
D136N[c]	1.10	0.10 ± 0.02	18 ± 1	100	48
E140Q[c]	1.10	0.27 ± 0.02	15 ± 1	150	45
D168N[c]	1.10	0.56 ± 0.02	21 ± 1	660	14
D174N	0.93	0.40 ± 0.05	35 ± 5	500	20
E185Q	1.10	0.14 ± 0.01	50 ± 4	500	20

[a] Complex I content in mitochondrial membranes is expressed as relative specific NADH:HAR activity that is not affected by mutations in the NUKM subunit. The complex I content of the plasmid complemented *nukm*::*LEU2* deletion strain (parental) was set to 1.00.

[b] To account for variations in complex I content in different batches of mitochondrial membranes, dNADH:DBQ activity was normalized to complex I content expressed as specific NADH:HAR activity. Determination of V_{max}, K_m, and I_{50} values for mutants in positions *Asp-99* and *Asp-115* was not possible. dNADH:DBQ activities of these two mutants were determined at 100 μm dNADH and 60 μm DBQ whereby the parental strain showed 0.3 $\mu mol\ min^{-1}\ mg^{-1}$.

[c] Data for mutants E89A, E89C, E89Q, D136N, E140Q, and D168N were taken from Ref. 8. In this earlier study V_{max} values were determined using *n*-nonylubiquinone as electron acceptor. DBQ and NBQ gave comparable K_m and V_{max} values for the parental strain.

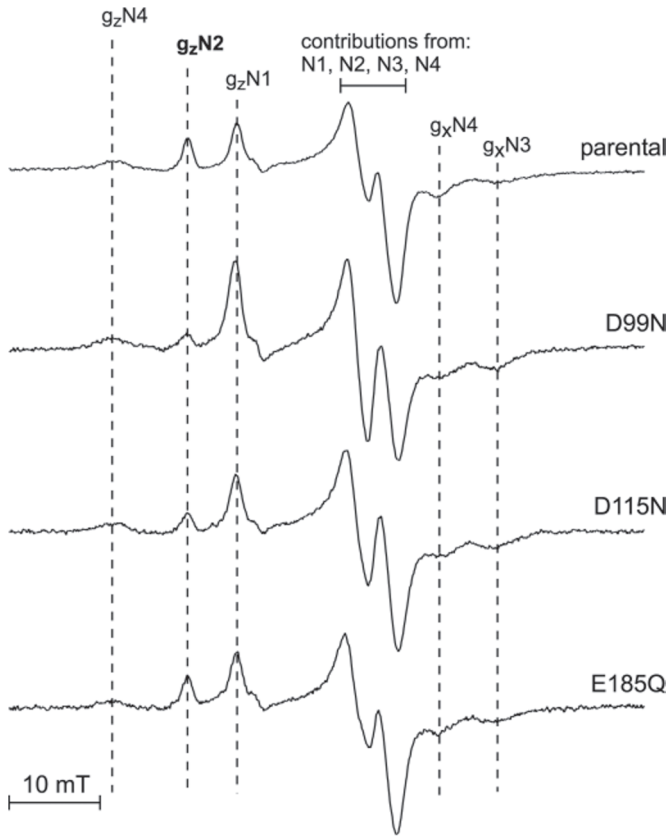

FIG. 2. **EPR spectra of purified complex I from parental and mutant strains.** EPR spectra of isolated complex I from parental and mutant strains reduced with NADH. The intensities of the spectra were scaled to the g_z signal intensity of cluster N1 recorded separately at 40 K for each sample. *Dotted lines* indicate field positions for g-values of individual clusters: g_zN4, 2.104; g_zN2, 2.051; g_zN1, 2.018; g_xN4, 1.892; g_xN3, 1.861. EPR conditions: microwave frequency 9.475 GHz, modulation amplitude 0.64 mT, microwave power 1 mW, temperature 12 K.

included here for comparison and completeness (see Table I). As a qualitative test for complex I assembly, mitochondrial membranes from each mutant were subjected to blue native polyacrylamide gel electrophoresis, and complex I content was quantified by NADH:HAR activity of mitochondrial membranes. All mutants analyzed in this study were found to have fully assembled complex I (data not shown), and its content in mitochondrial membranes was within the range commonly observed with the parental strain (Table I). The catalytic activity of complex I toward quinones was measured as specific dNADH:DBQ oxidoreductase activity and normalized to complex I content in the membranes. Table I summarizes the data obtained with mitochondrial membranes from all *Y. lipolytica* mutants and lists the K_m and V_{max} values for dNADH:DBQ activity and the I_{50} values for the complex I inhibitors DQA and rotenone.

Codon 99 in the *NUKM* open reading frame translates into a fully conserved aspartic acid (Fig. 1). Changing this carboxylate into its corresponding amide asparagine resulted in almost complete loss (<5% residual activity) of dNADH:DBQ oxidoreductase activity in the presence of saturating amounts of both substrates. Due to this very low activity, determination of K_m, V_{max}, and I_{50} values for complex I inhibitors was not possible. Affinity purification of complex I from mutant D99N was successful, but the yield in two independent purification experiments was only 25% as compared with the parental strain. As the content of complex I in membranes was only slightly lower that in the parental strain, the low purification yield suggested a somewhat lower stability of complex I in mutant D99N. The observation of decreased temperature stability of NADH:HAR oxidoreductase activity in D99N membranes was consistent with this interpretation (data not shown). This structural instability was also evident from the fact that in the first complex I preparation from this mutant, cluster N2 was not detectable by EPR spectroscopy whereas the spectra of all other visible clusters were unaffected. In the second batch of complex I from mutant D99N, the presence of iron-sulfur cluster N2 was clearly evident from EPR spectra recorded at 12 K and the g_z value for iron-sulfur cluster N2 was not shifted, indicating that the mutation had not influenced ligand geometry (Fig. 2). To compensate for different complex I concentrations all spectra were normalized to the N1 g_z signal intensity of the parental enzyme at 40 K (not shown). At this temperature cluster N1 can be measured selectively avoiding background effects from other overlapping iron-sulfur clusters, like iron-sulfur cluster S3 of complex II. At 12 K the signal of this cluster contributed significantly to the slightly shifted peak at the N1 field position, indicating that significant amounts of complex II were present as an impurity in the complex I preparation from mutant D99N. Using signal calibration at 40 K, the amplitude of the g_z signal of cluster N2 in complex I from the parental strain and mutant could still be compared showing that in the second batch of complex I from mutant D99N the amount of N2 was decreased by about 50%. The lowered cluster N2 content was also evident from the g_{xy} region of the EPR spectra, but because signals originating from all iron-sulfur clusters overlap in this field position this signal could not be used for quantitation. To test a more conservative mutation that left the carboxylic acid function at position 99 intact, we replaced the aspartic acid with glutamic acid: in terms of assembly and complex I content in mitochondrial membranes D99E did not show any significant difference compared with the parental strain or mutant D99N. Also dNADH:DBQ activities of D99E and D99N were comparable (< 5% of the wild type rate). As a more drastic mutation, we changed

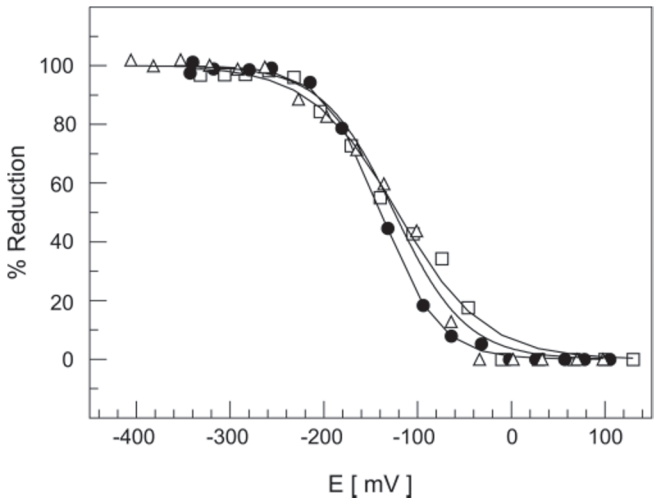

FIG. 3. **Redox titrations of iron-sulfur cluster N2 monitored by EPR spectroscopy.** ●, parental mitochondrial membranes, $E_{m,7}$ = −140 mV; △, mutant D99N, $E_{m,7}$ = −125 mV; □, mutant D115N, $E_{m,7}$ = −120 mV.

aspartic acid 99 into glycine. In membranes from mutant D99G, complex I was still fully assembled in normal amounts and dNADH:DBQ activity was as low as for mutants D99N and D99E.

A second fully conserved aspartic acid residue in the *NUKM* sequence codon 115 (Fig. 1) was mutagenized to give asparagine or glutamic acid. Both mutants, D115N and D115E, contained assembled complex I, but dNADH:DBQ oxidoreductase activities were found to be only ~8% of the wild type rate. Like for the Asp-99 mutants, this low activity made the determination of K_m, V_{max}, and I_{50} values for complex I inhibitors impossible. The purification of complex I from both mutants gave a yield of 39% for D115N and 35% for D115E as compared with the parental strain. Like in the case of mutant D99N, this low yield suggested some destabilization of complex I, which was also reflected in a slight decrease in temperature stability (data not shown). EPR spectroscopy of complex I isolated from D115N (Fig. 2) showed that the g_z values for clusters N1, N3, and N4 were not changed and that their relative amplitudes were comparable with complex I from the parental strain. Like in the case of D99N, the g_z signal for cluster N2 was not shifted, but a reduction in signal intensity by about 50% was observed. This was also evident from the g_{xy} region of the N2 spectrum. As for Asp-99, the aspartic acid in position 115 was also changed into glycine. Complex I content and assembly in mitochondrial membranes from mutant D115G was normal, and dNADH:DBQ oxidoreductase activity was not significantly different from D115N and D115E.

Based on these results we could not fully exclude the possibility that Asp-99 and Asp-115 form a pair of hydrogen bonds to iron-sulfur cluster N2, as in this case elimination of either residue still may have allowed assembly of the [Fe_4S_4] center. For this scenario, the midpoint potential of the redox center is predicted to change in the mutants due to the removal of one the hydrogen bonds. Therefore, we determined the midpoint potential of cluster N2 in membranes from mutants D99N and D115N. As shown in Fig. 3, the values of 120–130 mV for both mutants were not significantly different from that obtained for the parental strain.

A third fully conserved aspartate is located at position 174 (see Fig. 1). This position was changed into asparagine. Complex I content in membranes from mutant D174N was within the range commonly observed for the parental strain. V_{max} for DBQ and I_{50} values for rotenone and DQA were not significantly changed, whereas the K_m value for ubiquinone was slightly increased (Table I). No significant effects on complex I had been observed previously when the fourth fully conserved aspartate, Asp-168, had been changed into asparagine (Ref. 8 and Table I).

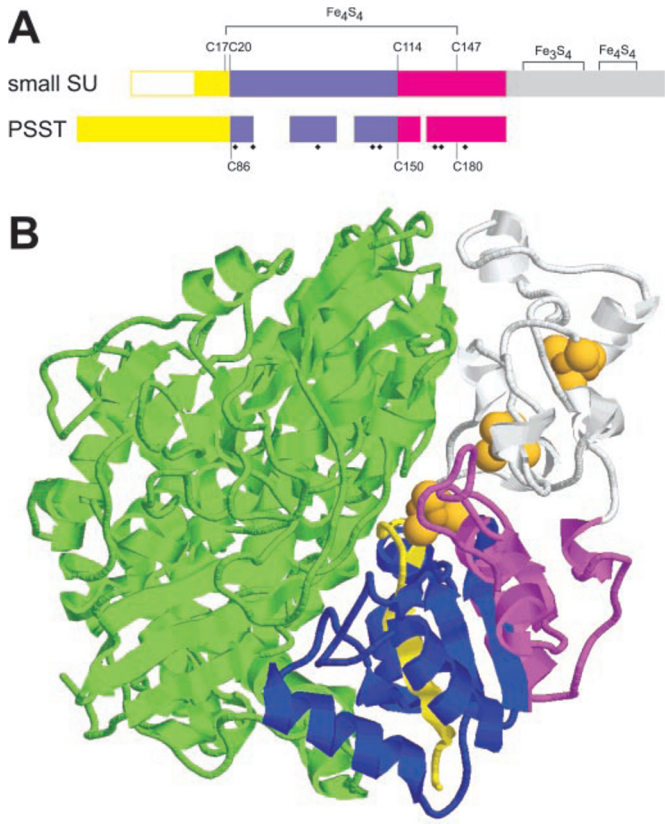

FIG. 4. **Domains of the small subunit of [NiFe] hydrogenase corresponding to functionally relevant domains within subunit PSST.** Comparison was based on the sequence and x-ray structure of [NiFe] hydrogenase from *Desulfovibrio fructosovorans*, Protein Data Bank code 1FRF (26). *A*, domain alignment between the small subunit of [NiFe] hydrogenase (*small SU*) and subunit PSST (*PSST*, *Y. lipolytica* numbering). The binding regions for the iron-sulfur-clusters are indicated by *brackets*. ♦, position of highly conserved acidic residues in subunit PSST; *C17*, *C20*, *C114*, and *C147*, cysteines ligating the proximal iron-sulfur cluster in hydrogenase; *C86*, *C150*, and *C180*, cysteines conserved in subunit PSST; *yellow*, N-terminal up to second cysteine ligating the proximal iron-sulfur cluster in hydrogenase. The part of the sequence symbolized by an *open box* is not contained in the 1FRF coordinate file; *blue*, region between second and third cysteine of small subunit; *magenta*, region downstream of third cysteine, retained in subunit PSST of complex I; *gray*, C-terminal, iron-sulfur cluster harboring domain of small subunit, missing in PSST subunit of complex I. *B*, schematic representation of the x-ray structure of [NiFe] hydrogenase. Mutations in the PSST subunit of complex I that have significant effects are clustered in the region corresponding to the domain shown in *blue*. See "Discussion" for further details. Iron-sulfur clusters are shown in *yellow space fill* representation. *Green*, large subunit, homologous to the 49 kDa subunit in complex I. *Other colors* as in *panel A*.

Two fully conserved glutamic acids can be identified in the sequences of complex I subunits homologous to subunit PSST (see Fig. 1), E89 and E185. Glutamate 89 has a position close to cysteine 86, and glutamate 185 is located near cysteine 180; both cysteines are possible ligands for cluster N2. Mutant E185Q exhibited a moderate 65% decrease in dNADH:DBQ activity. The K_m value for DBQ was increased about 2-fold, but I_{50} values for rotenone and DQA were the same as for the parental strain (Table I). The purification of complex I from mutant E185Q was successful, and the yield obtained from this mutant isolation was comparable with the parental strain. The EPR spectrum from E185Q was virtually indistinguishable

from spectra of parental complex I: there were no effects on positions of the g_z signals of clusters N1, N2, N3, and N4, and their intensities were also unaffected (Fig. 2). This is in contrast to mutants E89Q, E89C, and E89A that exhibited shifted g_z values and decreased signal intensities for iron-sulfur cluster N2 (8) and slightly lowered I_{50} values for DQA (Table I). Mutant E89Q also exhibited a reduced K_m value for ubiquinone. In the positions corresponding to codons 136 and 140 of the *NUKM* gene an acidic residue (Asp or Glu) is found in all known sequences of PSST homologous subunits. When these two amino acids were changed in their corresponding amides (8), ubiquinone reductase activity of complex I was found to be moderately decreased, and hypersensitivity to rotenone and slight resistance to DQA was observed (Table I).

DISCUSSION

By changing every one of eight conserved acidic residues in the PSST-homologous NUKM subunit of *Y. lipolytica* complex I, we have made an initial assessment of their role in complex I function. Two aspartates, Asp-99 and Asp-115, were found to be absolutely essential for complex I function as even the two most conservative exchanges possible, introducing an additional methylene group by changing them to glutamate or removing the charge by introducing the amide asparagine, resulted in almost complete loss of ubiquinone reductase activity. We could exclude by redox titration with membranes from mutants D99N and D115N that a shift in the midpoint potential of iron-sulfur cluster N2 was blocking electron transfer. Although mitochondrial membranes from all four mutants contained virtually normal amounts of complex I, a decrease in complex I stability became evident from lower yields during protein purification and a concomitant partial loss of iron-sulfur cluster N2. Even the rather drastic exchange of each of the aspartates to glycine still allowed normal assembly of complex I; residual activity and stability of complex I was practically the same as for the more conservative exchanges. The very similar effect of rather different amino acid exchanges in these two positions makes it tempting to speculate that in all cases a similar local change of a structural configuration occurred and that the resulting collapsed configuration was incompatible with ubiquinone reductase activity of complex I. As shown in our earlier study (8), the ligand field geometry of iron-sulfur cluster N2 is affected specifically when Glu-89 was exchanged with alanine, cysteine, or glutamine and mutations D136N and E140Q have significant effects on inhibitor binding (see Table I). Changing Asp-168, Asp-174, or Glu-185 to the corresponding amide had little or no effect on complex I.

EPR spectra of complex I from all mutants showed normal or in one case somewhat shifted spectra of iron-sulfur cluster N2. The possibility that Asp-99 and Asp-115 form a pair of hydogen bonds to iron-sulfur cluster N2 could be excluded as the midpoint potentials in membranes from mutants D99N and D115N were unchanged. Therefore, all conserved acidic residues in the PSST subunit can be excluded as fourth ligand of this redox-center.

A more detailed interpretation of the observed effects is difficult without a high-resolution structure of complex I. It has been demonstrated previously for mutants of the 49-kDa subunit, the homologue of the large hydrogenase subunit (15), that structural homologies to water-soluble [NiFe] hydrogenases for which x-ray structures are available (24–26) can be very useful to understand structure/function relationships in complex I. Our results suggest that also a comparison of the small subunit of water-soluble [NiFe] hydrogenases and the PSST subunit of complex I provides important clues (Fig. 4). Subunit PSST is much smaller than the small hydrogenase subunit because the C-terminal half that forms the domain harboring two of the three iron-sulfur clusters of hydrogenase is completely missing (Fig. 4*A*). Sequence conservation in the remaining part of the protein is rather weak, but three of the four cysteines that ligate the third, proximal cluster in the small hydrogenase subunit are conserved in subunit PSST (see Fig. 1), allowing a reasonable alignment of the sequences. Changing the conserved acidic residues around Cys-180 had very little effect on the function of complex I; the corresponding residues in the hydrogenase structure (Fig. 4, *magenta*) are found at the interface to the C-terminal iron-sulfur domain that is missing in subunit PSST. In contrast, Cys-86 and adjacent Glu-89 are predicted to be near the interface between PSST and the 49-kDa subunit; this position is consistent with the observed distortions of the ligand field of iron-sulfur custer N2 observed in mutants E89Q, E89C, and E89A (8). The four positions at which mutations had pronounced effects are located between Cys-86 and Cys-150. Although conservation between complex I subunits from different species was found to be very high in this part of the PSST subunit (36% identical residues between mammals and bacteria; see Fig. 1), this region has little similarity with the corresponding region of the small hydrogenase subunit (Fig. 4, *blue*) and is shortened by 30 amino acids (Fig 4*A*). This suggests that this part of the PSST subunit structure is rather different from the small subunit of hydrogenase, but it still seems reasonable to assume that the position of this domain relative to the iron-sulfur cluster ligating cysteines has remained the same. It is important to note that based on this proposal this part of the PSST subunit would be predicted to be adjacent to regions of the 49-kDa subunit (Fig. 4, *green*) in which mutations causing inhibitor resistance (14, 27) and functional defects have been identified.[2] Conservative mutations of acidic amino acids in the region between Cys-86 and Cys-150 caused almost complete loss of catalytic activity (Asp-99 and Asp-115) or significant hypersensitivity to rotenone and resistance to DQA (Asp-136 and Glu-140). This fits well with the observation that mutation V119M was found previously to cause a 50% decrease in activity and a moderate hypersensitivity for DQA (28). We had reconstructed this mutation in *Y. lipolytica* because the homologous V122M substitution in the human *NUDFS7* gene had been reported to cause Leigh-Syndrome (29). We conclude that this part of the PSST subunit represents another functionally important domain of the catalytic core of complex I.

Acknowledgments—We thank Andrea Böttcher, Franz-Josef Streb, Gudrun Beyer, and Jolanta Maria Brzoska for excellent technical assistance and Dr. Volker Zickermann for help and useful suggestions in protein purification.

REFERENCES

1. Carroll, J., Fearnley, I. M., Shannon, R. J., Hirst, J., and Walker, J. E. (2003) *Mol. Cell. Proteomics* **2,** 117–126
2. Wikström, M. K. F. (1984) *FEBS Lett.* **169,** 300–304
3. Brandt, U., Kerscher, S., Dröse, S., Zwicker, K., and Zickermann, V. (2003) *FEBS Lett.* **545,** 9–17
4. Magnitsky, S., Toulokhonova, L., Yano, T., Sled, V. D., Hagerhall, C., Grivennikova, V. G., Burbaev, D. S., Vinogradov, A. D., and Ohnishi, T. (2002) J. *Bioenerg. Biomembr.* **34,** 193–208
5. Friedrich, T. (1998) *Biochim. Biophys. Acta* **1364,** 134–146
6. Duarte, M., Populo, H., Videira, A., Friedrich, T., and Schulte, U. (2002) *Biochem. J.* **364,** 833–839
7. Ohnishi, T. (1998) *Biochim. Biophys. Acta* **1364,** 186–206
8. Ahlers, P., Zwicker, K., Kerscher, S., and Brandt, U. (2000) *J. Biol. Chem.* **275,** 23577–23582
9. Chevallet, M., Dupuis, A., Issartel, J. P., Lunardi, J. L., van Belzen, R., and Albracht, S. P. J. (2003) *Biochim. Biophys. Acta* **1557,** 51–66
10. Rasmussen, T., Scheide, D., Brors, B., Kintscher, L., Weiss, H., and Friedrich, T. (2001) *Biochem.* **40,** 6124–6131
11. Schuler, F., Yano, T., Di Bernardo, S., Yagi, T., Yankovskaya, V., Singer, T. P., and Casida, J. E. (1999) *Proc. Natl. Acad. Sci. U. S. A.* **96,** 4149–4153
12. Sauter, M., Böhm, R., and Böck, A. (1992) *Mol. Microbiol.* **6,** 1523–1532

[2] L. Grgic, K. Zwicker, N. Kashani-Poor, S. Kerscher, and U. Brandt, manuscript in preparation.

13. Albracht, S. P. J. (1993) *Biochim. Biophys. Acta* **1144,** 221–224
14. Kashani-Poor, N., Zwicker, K., Kerscher, S., and Brandt, U. (2001) *J. Biol. Chem.* **276,** 24082–24087
15. Kerscher, S., Kashani-Poor, N., Zwicker, K., Zickermann, V., and Brandt, U. (2001) *J. Bioenerg. Biomembr.* **33,** 187–196
16. Kerscher, S., Eschemann, A., Okun, P. M., and Brandt, U. (2001) *J. Cell Sci.* **114,** 3915–3921
17. Kashani-Poor, N., Kerscher, S., Zickermann, V., and Brandt, U. (2001) *Biochim. Biophys. Acta* **1504,** 363–370
18. Kerscher, S., Dröse, S., Zwicker, K., Zickermann, V., and Brandt, U. (2002) *Biochim. Biophys. Acta* **1555,** 83–91
19. Zickermann, V., Bostina, M., Hunte, C., Ruiz, T., Radermacher, M., and Brandt, U. (2003) *J. Biol. Chem.* **278,** 29072–29078
20. Schägger, H. (2003) in *Membrane Protein Purification and Crystallization: A Practical Guide* (Hunte, C., von Jagow, G., and Schägger, H., eds) pp. 105–130, Academic Press, San Diego, CA
21. Djafarzadeh, R., Kerscher, S., Zwicker, K., Radermacher, M., Lindahl, M., Schägger, H., and Brandt, U. (2000) *Biochim. Biophys. Acta* **1459,** 230–238
22. Dutton, P. L. (1978) *Methods Enzymol.* **LIV,** 411–435
23. Sled, V. D., and Vinogradov, A. D. (1993) *Biochim. Biophys. Acta* **1141,** 262–268
24. Rousset, M., Montet, Y., Guigliarelli, B., Forget, N., Asso, M., Bertrand, P., Fontecilla-Camps, J. C., and Hatchikian, E. C. (1998) *Proc. Natl. Acad. Sci. U. S. A.* **95,** 11625–11630
25. Volbeda, A., Charon, M. H., Piras, C., Hatchikian, E. C., Frey, M., and Fontecilla-Camps, J. C. (1995) *Nature* **373,** 580–587
26. Montet, Y., Amara, P., Volbeda, A., Vernede, X., Hatchikian, E. C., Field, M. J., Frey, M., and Fontecilla-Camps, J. C. (1997) *Nature Struct. Biol.* **4,** 523–526
27. Prieur, I., Lunardi, J., and Dupuis, A. (2001) *Biochim. Biophys. Acta* **1504,** 173–178
28. Ahlers, P., Garofano, A., Kerscher, S., and Brandt, U. (2000) *Biochim. Biophys. Acta* **1459,** 258–265
29. Triepels, R., Van den Heuvel, L. P., Loeffen, J. L., Buskens, C. A., Smeers, R. J. P., Rubio-Gozalbo, M. E., Budde, S. M. S., Mariman, E. C. M., Wijburg, F. A., Barth, P. G., Trijbels, J. M., and Smeitink, J. A. (1999) *Ann. Neurol.* **45,** 787–790